DINAME 2023 - Proceedings of the XIX International Symposium on Dynamic Problems of Mechanics,
A.S. De Paula, A.T. Fabro and M.R. Machado (Editors), ABCM.
Pirenópolis, Go, Brazil, February 26th to March 3rd, 2023

Acoustic characterization of porous ceramic produced via freeze-casting using DMSO as solvent.

T.S.da N. Guenka[1], **M.R. Machado**[1], **A.M.A. Silva**[1], **and M.A. A. Nunes**[2]

[1] UnB, Department of Mechanical Engineering, Campus Universitário Darcy Ribeiro, Asa Norte, Brasília-DF, CEP 70910-900

[2] UnB, Department of Automotive Engineering, Faculdade UnB Gama - FGA,Área Especial de Indústria Projeção A,Setor Leste, Gama, CEP 72.444-240

Abstract: Freeze-cast ceramics, polymers and even metals have recently attracted attention for their sound propagation characteristics, given their inherent controllable porosity associated with many different materials used in this fabrication route. This study used Dimethyl Sulfoxide (DMSO) as a solvent and alumina (corundum)/magnesium oxide (periclase) ceramics to produce samples. The impedance, reflection and sound absorption coefficients measured with an impedance tube are used to calibrate the Johson-Champoux-Allard-Lafarge (JCAL) model parameters through least squares curve fitting. These calibrated parameters are then investigated based on Scanning Electron Microscopy (SEM) images and porosity assessment using archimedes principle. A good sound absorption coefficient was found throughout the studied frequency range, although the correlation between found JCAL parameters and the material characterization results is still under investigation.

Keywords: Sound Absorption, Porous Material, Ceramic, DMSO, Freeze-Casting

INTRODUCTION

As challenges in noise control arise in diverse engineering applications daily, the need for a variety of solutions suitable for increasingly challenging problems is soaring. Within the realm of porous materials for SA applications, ceramics have been limited investigation for this application. However, ceramic materials properties are dissonant from traditional SA materials, e.g. polyurethane (PU) and fibrous materials, because of their high hardness and brittleness. Therefore, ceramics unique properties are excellent materials to work under a chemically aggressive atmosphere, high temperature, and thermal shock.

Associated with the freeze-casting method, ceramics with controlled macroporosity can be obtained reliable pore morphology based on the control of process parameters, such as solid loading, freezing temperature (Deville, 2008) and the freezing crystal growth and shape of the solvent may also determine the geometry of the pores (Deville, 2010). A few authors have studied the influence of freeze-casting (and similar methods) parameters on porous ceramics acoustic absorption characteristics such as (Du et al., 2020) and (Carlesso et al., 2013), showing the potential of the method for fabrication of such materials.

This paper evaluated the sound absorption of aluminium oxide/magnesium oxide samples produced via freeze-casting using DMSO as a solvent. For better analysis, the Johnson-Champoux-Allard-Lafarge (JCAL) model was used for calibration of its parameters and consequent correlation to its microstructure. Although DMSO has been investigated as a solvent for this method, some studies have shown it produces ladder-type morphology (Chu et al., 2015). Our investigation shows fair values for the sound absorption coefficient throughout the studied frequency band, although the found parameters have an unclear relation to the microstructure, which is still under investigation.

METHODS

FREEZE-CASTING

The freeze-casting process consists on the preparation of a slurry containing the solid components of the sample dispersed in a solvent. Such slurry is then frozen by an externally applied temperature gradient. The nucleation of solid crystals generates a freezing front that pushes the solid content, creating a structure consisting of connected solid solvent crystals with agglomerated solid content in between such crystals. Then, the solvent is sublimated and the remaining structure, consisting of a replica of the solidified solvent, is subsequently sintered (Deville, 2008).

For the monoliths production, the used starting powders were CT3000SG α-Al_2O_3 (99.8 wt %/ Almatis Brazil) and Magnesium Oxide ($\geq$ 99 % trace metals basis, -325 mesh, Sigma Aldrich). The used dispersant was citric acid (Sigma Aldrich, 99,5 %) and the solvent was DMSO (Dinamica). The solvent and dispersant were mixed using magnetic stirring until dissolution was observed, then the starting powders were added and mixed for a predetermined period. After mixing, the slurry was poured inside a mold placed on top of a copper cold finger with controlled constant temperature. Freezing was conducted in such way to promote unidirectional freezing and consequently aligned pore structure. When complete freezing of the sample was observed, it was demolded and set in a sample holder for the freeze-drying process. Freeze-drying is necessary to remove the crystallized solvent without affecting the formed pore channels. Finally, the sample is sintered in an oven and sanded to reach the dimensions appropriate to the impedance tube testing.

ACOUSTIC MODELING

The semi-phenomenological JCAL model was used to model the ceramic samples' acoustic properties. Johnson, Koplik and Dashen (1987) originally proposed an isotropic porous material model describing their complex equivalent fluid density of a rigid (motionless). Then later, their theory was complemented with the model by Champoux and Allard (Champoux & Allard, 1991) that further elaborated the equivalent bulk modulus dependence on frequency for the same materials. Finally, Lafarge et al. (Lafarge, Lemarinier, Allard, & Tarnow, 1997) suggested changes to the bulk modulus equation to correct the description of low-frequency thermal phenomena in the previous models, leading to the JCAL model. A complete description of the model can be found in (Allard & Atalla, 2009). The equations for the equivalent density and bulk modulus, both functions of sound frequency ω, are given as:

$$\rho_{eq}(\omega) = \frac{\rho_f \alpha_\infty}{\phi}\left[1 - \frac{\nu_f \phi}{\omega k_0 \alpha_\infty}\sqrt{1 + i\frac{\omega}{\nu_f}\left(\frac{2\alpha_\infty k_0}{\phi \Lambda}\right)^2}\right] \tag{1}$$

$$K_{eq}(\omega) = \frac{\gamma P_0}{\phi}\left\{\frac{\gamma(\gamma-1)}{1 - i\frac{\phi \nu'_f}{\omega k'_0}\sqrt{\frac{i\omega}{\nu'_f}\left(\frac{2k'_0}{\Lambda'\phi}\right)^2 + 1}}\right\}^{-1}. \tag{2}$$

In equations 1 and 2, P_0 is the atmospheric pressure, ρ_f is the saturating fluid density, γ is its specific heat ratio, ν_f its kinematic viscosity and ν'_f is defined as ν_f/Pr, where Pr is the Prandtl number. In addition to the saturating fluid properties, the JCAL model is based on six geometrical parameters of the porous medium, specific to the pore morphology. These are the open porosity ϕ , the high frequency limit of the tortuosity α_∞, static viscous permeability k_0 (given by the ratio $\frac{\mu}{\sigma}$ between the fluid dynamic viscosity μ and the static air flow resistivity σ, static thermal permeability k'_0 and the viscous and thermal characteristic lengths Λ and Λ', respectively. From the equivalent fluid properties, its characteristic impedance Z_c and its complex wave number k are obtained:

$$Z_c = \sqrt{(K_{eq}\rho_{eq})}, \tag{3}$$

$$k = \sqrt{\omega(\rho_{eq}/K_{eq})}. \tag{4}$$

Finally, from equations 3 and 4 it is possible to determine the surface impedance of a sample with thickness d:

$$Z = -i\frac{Z_c}{\phi}\mathrm{cotg}(kd). \tag{5}$$

By using the surface impedance of the sample, the reflection coefficient r of the sample is determined and the sample acoustic absorption α can be acquired:

$$r(\omega) = \frac{Z(\omega) - Z_f}{Z(\omega) + Z_f}, \tag{6}$$

$$\alpha = 1 - |r|^2. \tag{7}$$

Inverse characterization is the estimation of the model parameters using an inverse problem/optimization approach (Atalla & Panneton, 2005). For this purpose, a suitable objective function based on one of a sample's measured acoustic properties is defined and minimized. Once a convergence criterion for the minimization process is achieved, the parameter estimates are obtained. The used objective function is:

$$R(\mathrm{a}) = 0.5\sum_{\omega}\frac{1}{w}|Z^{exp}(\omega) - Z(\omega,\mathrm{a})|, \tag{8}$$

where $Z^{exp}(\omega)$ is the obtained experimental sample surface impedance at frequency ω, w is the standard deviation for each experimentally obtained impedance value, $Z(\omega,\mathrm{a})$ is the obtained modelled surface impedance for the vector of model parameters a at the same frequency. Notice that the objective function only uses data points obtained for different frequencies without using other possible setups that can increase the size of the dataset. Such as different air gaps

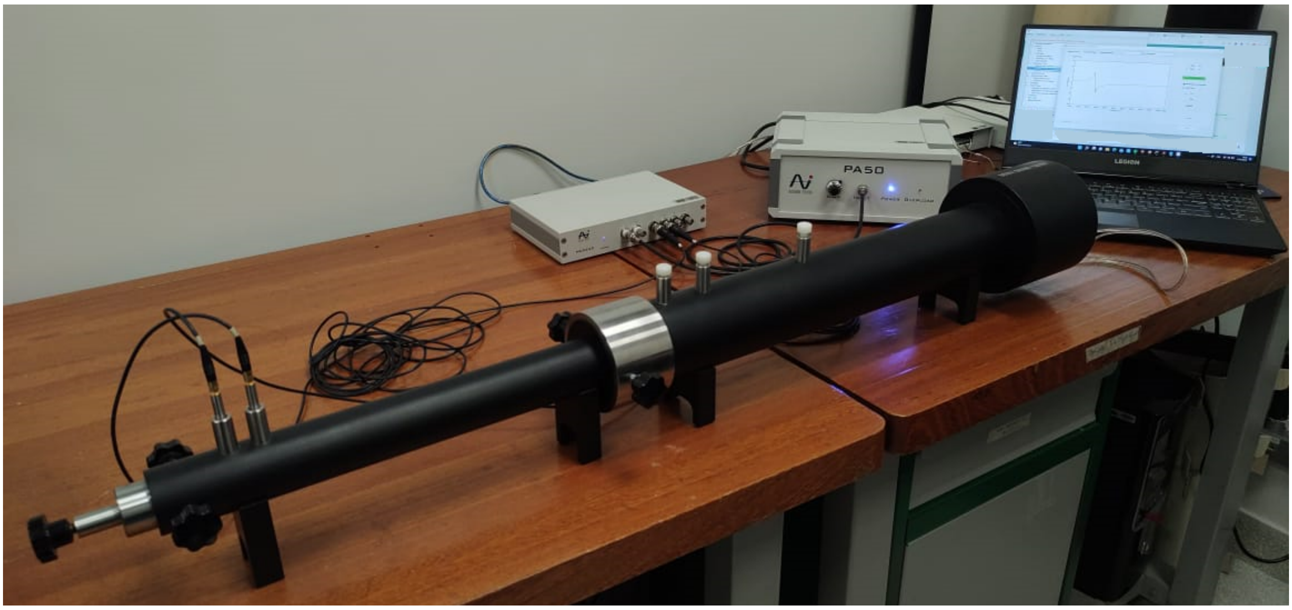

Figure 1: Acoustic characterization equipment

(Zieliński, 2015) (Roncen, Fellah, & Ogam, 2022) or incidence angles (De Ryck et al., 2008), simply due to equipment limitations.

There are different numerical optimization methods available for solution of the problem, many already implemented in commercial or open-source packages. A version of the Levenberg-Marquardt (Levenberg, 1944) (Marquardt, 1963) algorithm was implemented and the parametric version of the JCAL model presented in (Zieliński, 2015) was used as the numerical surface impedance model for the samples.

ACOUSTIC CHARACTERIZATION

For the experimental acoustic characterization of the samples, the BWSA SW466 impedance tubes were used, consisting of two tubes of different internal diameters: one with 30 mm and another with 60 mm internal diameter. The smaller tube is used for higher frequencies, with a range of 1000-6300 Hz, while the larger yields result for lower frequencies from 100 Hz - 2500 Hz. The MC3242 data acquisition system was coupled with the PA 50 amplifier and two microphones. Additionally, the employed VA-Lab4 software generates the signal for the sound source. Also, it gives the acquired results for acoustic impedance, absorption and reflection coefficients, based on the transfer function method described in ISO 10534:2. Figure 1 shows the impedance tube setup.

The production of $\varnothing = 60$ mm samples using the freeze-casting method is very resource demanding, considering the amount of suspension necessary to fill the cavity for such samples. Moreover, the replicability of the properties of the $\varnothing = 30$ mm sample for a $\varnothing = 60$ mm sample is difficult given the need for, in the freeze-casting setup, a larger diameter cold finger which would replicate precisely the temperature gradient obtained with the $\varnothing = 30$ mm sample cold finger, besides the needed higher slurry pouring speed among other factors. The confection of both samples using this method would likely result in samples with, in addition to different diameters, different pore morphologies and thus different acoustic properties. Thus, the produced samples were limited to $\varnothing = 30$ mm and consequently the analyzed frequency band was 1000 Hz - 6300 Hz.

RESULTS

Table 1 shows the sample fabrication parameters, namely the slurry solid concentration (in volume), the used ratio (in mass) between the starting powders that were added to the slurry, concentration of the dispersant relative to the total added solid mass and freezing temperature. The produced sample's height was $h = 20$ mm.

Solvent concentration	Solid Concentration	Dispersant concentration	Freezing Temp.
80 vol% DMSO/ 20 vol% solid	72 wt% Al_2O_3/28 wt% MgO	2 wt% solid mass	-150 °C

Table 1: Fabrication specifications of the characterized sample

The experimentally obtained surface impedance ratios and the numerically fitted model ratios are shown in Fig. 2. Both components of the numerically obtained impedance follow a similar trend and match the range of the measured values,

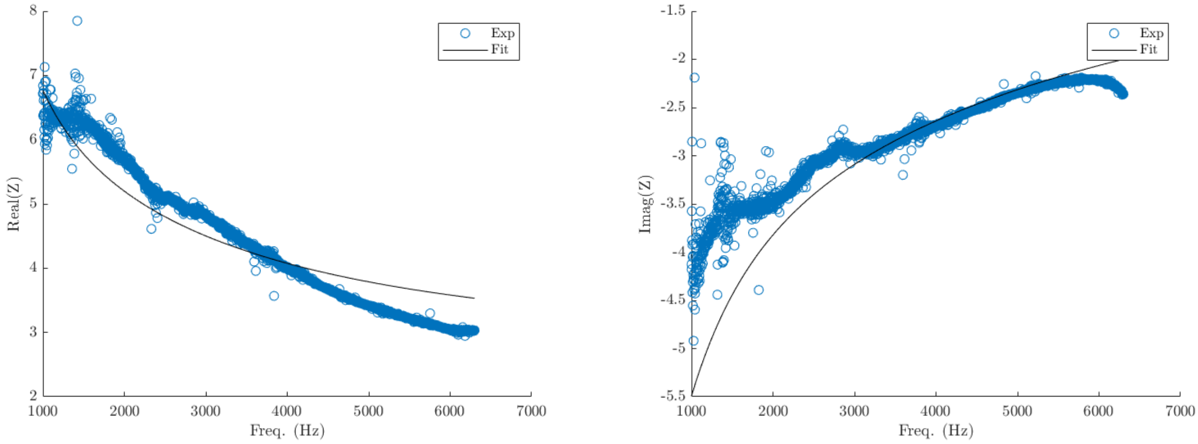

(a) (b)

Figure 2: Obtained fits of the real and imaginary parts of the impedance ratio.

sample	ϕ	α_∞	λ (m)	λ' (m)	σ (Nsm^{-4})	k'_0 (m^2)
72 wt% Al2O3/28 wt% MgO	0,9681	5,5991	3,3039e-5	2,0682e-4	7,0525e+5	1,8319e-9

Table 2: Sample's numerically found acoustic properties.

notwithstanding a visually poor match between experimental and calibrated results. Figure 3 shows the comparison between the experimentally obtained and the calibrated model sound absorption coefficient curve.

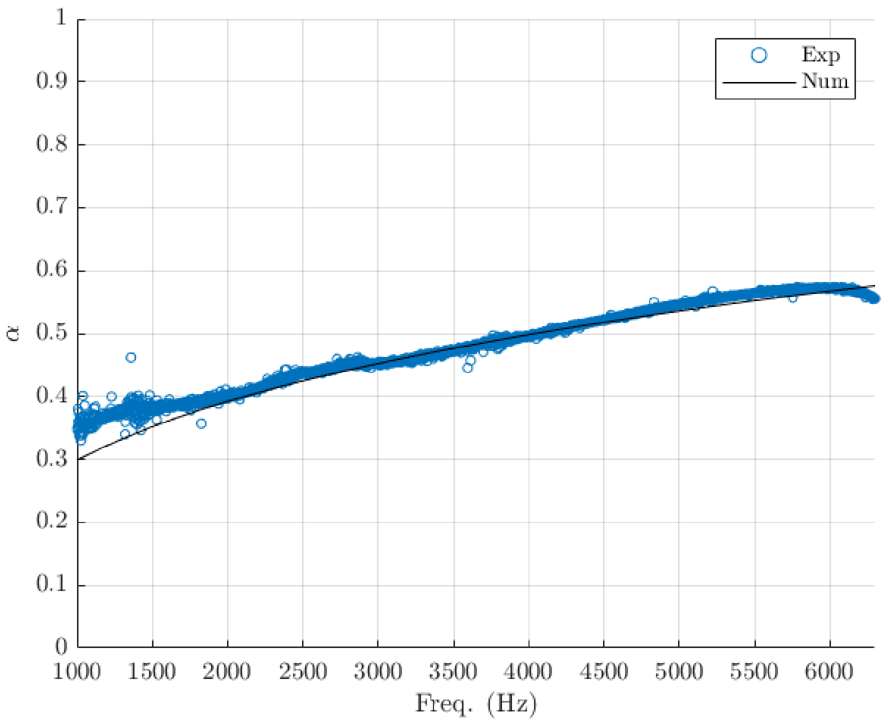

Figure 3: Experimental and calibrated sound absorption coefficient curves.

Table 2 shows the JCAL calibrated parameters based on the shown impedance curves. A few of the obtained values draw attention: the high frequency limit of the tortuosity shows a high value compared to other materials in literature (Zieliński, 2015) and calculations for theoretical pore morphologies (Allard & Atalla, 2009), possibly indicating a pore

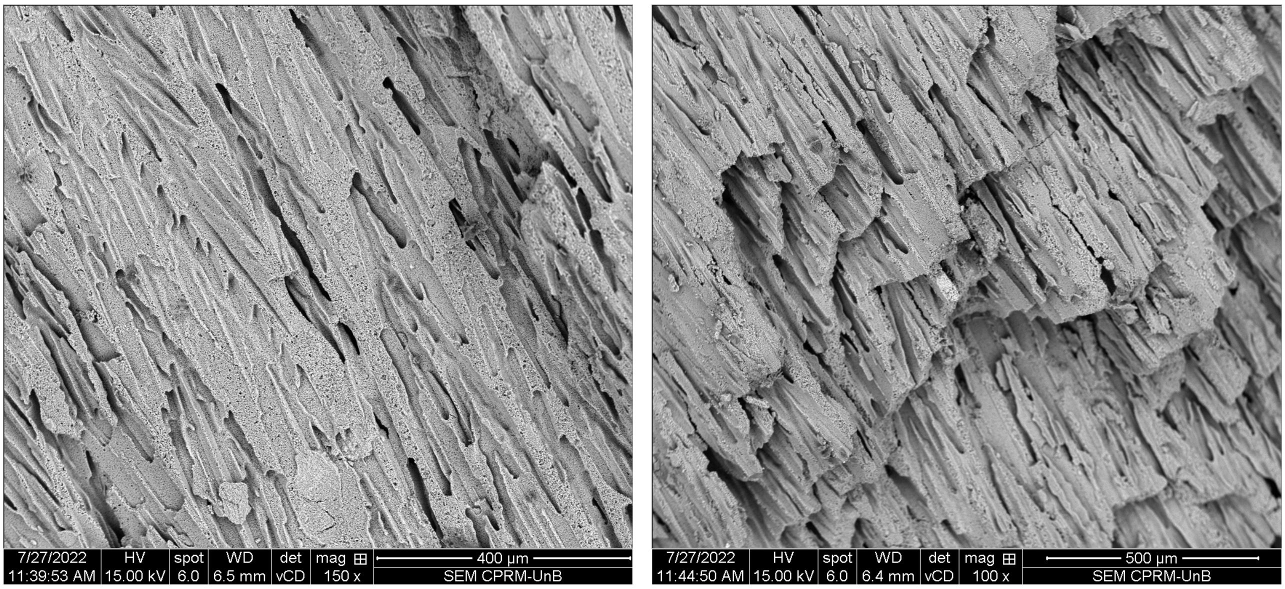

(a) (b)

Figure 4: SEM images of the ceramic sample.

double or multi scale material (Boutin, Royer, & Auriault, 1998) being modeled with a single scale porosity model. Also, Archimedes principle was used to measure open porosity of the sample obtaining a value of 67,4 %, while the calibrated porosity model shows 96,81 %, possibly indicating an error either in the physical measurement or in the model chosen for calibration.

Figure 4 shows two images of a cleaved monolith obtained through SEM, Fig. 4a being of the inner bulk of the sample, and Fig. 4b being of the outer surface (the flat surface that faces the sound source in the impedance tube testing). In both figures, the formation of complex channels with intricate geometry is observed. The pores have a clear alignment resultant of the unidirectional freezing, even though the crystals grew in such way to form a triangular alignment. This morphology might be related to the high values of estimated tortuosity high frequency limit. Additionally, there are different pore connection sizes that may both influence on tortuosity and pore scale, possibly causing pressure diffusion effects (Venegas & Boutin, 2018) (Langlois, Trinh, & Perrot, 2019). Another factor that may influence the wave propagation through the sample is the existence of sharp edge protuberances visible inside the channel and and apparent roughness of the surface of the observed pores, both influential in the fluid flow (Cortis, Smeulders, Guermond, & Lafarge, 2003) and consequently sound absorption.

CONCLUSION

In order to evaluate the potential of a porous material fabrication technique applied to a specific ceramic composition for acoustic applications, we performed a experimental and numerical study on a ceramic sample produced via freeze-casting. The acoustic absorption of the sample was obtained using impedance tube testing and showed fair absorption throughout the analyzed frequency band. Sample surface impedance was also obtained from the same experiment and was used to calibrate the parameters of the JCAL model for rigid frame porous acoustic materials. Such calibration was done using least squares approach associated with Levenberg-Marquardt method. The calibrated parameters show that the single porosity model may be inadequate, due to the obtained parameter values that extrapolate those observed in conventional acoustic material. SEM images of the sample‘s microstructure are analyzed and the possible relations between microstructure and acoustic parameters were discussed.

The studied material has interesting features and the obtained acoustic absorption is promising. Future research on the possible effects of multi-scale porosity, pore morphology and surface roughness is necessary for better control and optimization of the absorption properties.

RESPONSIBILITY NOTICE

The author(s) is (are) the only responsible for the printed material included in this paper.

REFERENCES

Allard, J. F., & Atalla, N. (2009). *Propagation of sound in porous media: Modelling sound absorbing materials*. John Wiley & Sons, Ltd.

Atalla, Y., & Panneton, R. (2005, 03). Inverse acoustical characterization of open cell porous media using impedance tube measurements. *Canadian Acoustics - Acoustique Canadienne*, *33*.

Boutin, C., Royer, P., & Auriault, J. (1998). Acoustic absorption of porous surfacing with dual porosity. *International Journal of Solids and Structures*, *35*(34), 4709-4737. Retrieved from `https://www.sciencedirect.com/science/article/pii/S0020768398000912` doi: https://doi.org/10.1016/S0020-7683(98)00091-2

Carlesso, M., Giacomelli, R., Krause, T., Molotnikov, A., Koch, D., Kroll, S., ... Rezwan, K. (2013). Improvement of sound absorption and flexural compliance of porous alumina-mullite ceramics by engineering the microstructure and segmentation into topologically interlocked blocks. *Journal of the European Ceramic Society*, *33*(13), 2549-2558. Retrieved from `https://www.sciencedirect.com/science/article/pii/S0955221913002458` doi: https://doi.org/10.1016/j.jeurceramsoc.2013.05.006

Champoux, Y., & Allard, J. (1991). Dynamic tortuosity and bulk modulus in air-saturated porous media. *Journal of Applied Physics*, *70*(4), 1975-1979. Retrieved from `https://doi.org/10.1063/1.349482` doi: 10.1063/1.349482

Chu, Y., Lu, Z., Li, J., Zhu, Y., Zhang, S., & Chen, J. (2015). Preparation of poly (l-lactic acid) with aligned structures by unidirectional freezing. *Polymers for Advanced Technologies*, *26*(6), 606-612. Retrieved from `https://onlinelibrary.wiley.com/doi/abs/10.1002/pat.3493` doi: https://doi.org/10.1002/pat.3493

Cortis, A., Smeulders, D. M. J., Guermond, J. L., & Lafarge, D. (2003). Influence of pore roughness on high-frequency permeability. *Physics of Fluids*, *15*(6), 1766-1775. Retrieved from `https://aip.scitation.org/doi/abs/10.1063/1.1571545` doi: 10.1063/1.1571545

De Ryck, L., Lauriks, W., Leclaire, P., Groby, J. P., Wirgin, A., & Depollier, C. (2008). Reconstruction of material properties profiles in one-dimensional macroscopically inhomogeneous rigid frame porous media in the frequency domain. *The Journal of the Acoustical Society of America*, *124*(3), 1591-1606. Retrieved from `https://doi.org/10.1121/1.2959734` doi: 10.1121/1.2959734

Deville, S. (2008). Freeze-casting of porous ceramics: A review of current achievements and issues. *Advanced Engineering Materials*, *10*(3), 155-169. Retrieved from `https://onlinelibrary.wiley.com/doi/abs/10.1002/adem.200700270` doi: https://doi.org/10.1002/adem.200700270

Deville, S. (2010, Mar 17). Freeze-casting of porous biomaterials: Structure, properties and opportunities. *Materials*, *3*(3), 1913-1927. Retrieved from `https://www.ncbi.nlm.nih.gov/pmc/articles/PMC5445887/` (PMC5445887[pmcid]) doi: 10.3390/ma3031913

Du, Z., Yao, D., Xia, Y., Zuo, K., Yin, J., Liang, H., & Zeng, Y.-P. (2020). The sound absorption performance of the highly porous silica ceramics prepared using freeze casting method. *Journal of the American Ceramic Society*, *103*(10), 5990-5998. Retrieved from `https://ceramics.onlinelibrary.wiley.com/doi/abs/10.1111/jace.17300` doi: https://doi.org/10.1111/jace.17300

Lafarge, D., Lemarinier, P., Allard, J. F., & Tarnow, V. (1997). Dynamic compressibility of air in porous structures at audible frequencies. *The Journal of the Acoustical Society of America*, *102*(4), 1995-2006. Retrieved from `https://doi.org/10.1121/1.419690` doi: 10.1121/1.419690

Langlois, V., Trinh, V. H., & Perrot, C. (2019, Jul). Electrical conductivity and tortuosity of solid foam: Effect of pore connections. *Phys. Rev. E*, *100*, 013115. Retrieved from `https://link.aps.org/doi/10.1103/PhysRevE.100.013115` doi: 10.1103/PhysRevE.100.013115

Levenberg, K. (1944). A method for the solution of certain non-linear problems in least squares. *Quarterly of Applied Mathematics*, *2*(2), 164–168. Retrieved 2022-05-17, from `http://www.jstor.org/stable/43633451`

Marquardt, D. W. (1963). An algorithm for least-squares estimation of nonlinear parameters. *Journal of the Society for Industrial and Applied Mathematics*, *11*(2), 431–441. Retrieved 2022-05-17, from `http://www.jstor.org/stable/2098941`

Roncen, R., Fellah, Z. E. A., & Ogam, E. (2022). Addressing the ill-posedness of multi-layer porous media characterization in impedance tubes through the addition of air gaps behind the sample: Numerical validation. *Journal of Sound and Vibration*, *520*, 116601. Retrieved from `https://www.sciencedirect.com/science/article/pii/S0022460X21006131` doi: https://doi.org/10.1016/j.jsv.2021.116601

Venegas, R., & Boutin, C. (2018). Enhancing sound attenuation in permeable heterogeneous materials via diffusion processes. *Acta Acustica united with Acustica*, *104*(4), 623–635. doi: 10.3813/aaa.919202

Zieliński, T. G. (2015). Normalized inverse characterization of sound absorbing rigid porous media. *The Journal of the Acoustical Society of America*, *137*(6), 3232-3243. Retrieved from https://doi.org/10.1121/1.4919806 doi: 10.1121/1.4919806